

Time delayed electroluminescence overshoot in single layer polymer light-emitting diodes due to electrode luminescence quenching

J. M. Lupton

School of Physics and Astronomy, University of St. Andrews, St. Andrews, Fife KY16 9SS, United Kingdom, and Department of Physics, University of Durham, South Road, Durham DH1 3LE, United Kingdom

V. R. Nikitenko

Institut für Physikalische Chemie, Makromolekulare Chemie und Kernchemie und Zentrum für Materialwissenschaften, Philipps Universität, D-35032 Marburg, Germany

I. D. W. Samuel^{a)}

School of Physics and Astronomy, University of St. Andrews, St. Andrews, Fife KY16 9SS, United Kingdom and Department of Physics, University of Durham, South Road, Durham DH1 3LE, United Kingdom

H. Bässler

Institut für Physikalische Chemie, Makromolekulare Chemie und Kernchemie und Zentrum für Materialwissenschaften, Philipps Universität, D-35032 Marburg, Germany

(Received 24 April 2000; accepted for publication 11 October 2000)

We investigate the transient response of single layer polymer light-emitting diodes (LEDs) based on poly[2-methoxy, 5-(2'-ethyl-hexyloxy)-1,4-phenylene vinylene] (MEH-PPV). An electroluminescence overshoot is observed between 1 and 2 μ s after turning off the voltage pulse, depending on temperature. We attribute the delay between overshoot and voltage turnoff to detrapping of majority charge carriers at the polymer/cathode interface. Due to the luminescence quenching zone of the metal the luminescence is found to decrease rapidly after the voltage is switched off, but then rise again to up to a third of the steady state value. The overshoot is found to be independent of the applied bias, but is strongly influenced by temperature and pulse length, indicating a trapping process in interfacial traps is responsible for the effect. The overshoot area corresponds to the charge located on interfacial traps near the cathode and scales as a power law with the pulse length. Our findings demonstrate the presence of extrinsic traps in MEH-PPV devices and highlight the importance of distinguishing between the effects of extrinsic and intrinsic traps in polymer LEDs. Spatial correlations of electrons and holes due to their mutual Coulombic field also appear to be important. © 2001 American Institute of Physics. [DOI: 10.1063/1.1331066]

I. INTRODUCTION

Over the past decade, polymer light-emitting diodes (LEDs) have been the focus of intense scientific interest, which has led to great advances regarding materials, device fabrication, and device performance.¹ Although organic electroluminescence (EL) is in principle straightforward to describe, the macroscopic device parameters of these submicron scale structures are hard to predict quantitatively. In polymer LEDs, both injection and transport effects govern the current-voltage characteristics as well as light emission and efficiency. We present transient EL on single layer LEDs made of the polymer MEH-PPV. Transient EL has frequently been used as a tool to study device properties,²⁻⁸ both under low current cw conditions,²⁻⁵ and under high excitation density.^{6,7} It can be used to obtain a dispersion parameter which is related to structural disorder⁸ as well as information on charge carrier dynamics⁷ and trapping.³ Transient measurements are of great relevance to the development of passively addressed displays in which the peak

brightness of a pixel is generally much greater than the brightness of the display. Pulsed EL is also important for obtaining high excitation densities that will be needed for polymer lasers.⁷ We present data on an overshoot effect in single layer LEDs which we are able to explain by invoking the effect of an interfacial insulating layer on electron-hole correlation and the influence of geminate recombination on carrier diffusion.

II. EXPERIMENT

MEH-PPV LEDs were prepared on ITO substrates which had previously been masked, etched, and cleaned in an ultrasonic bath of acetone and isopropanol. MEH-PPV was spin coated from a chlorobenzene solution onto the substrate at spin speeds of typically 1000 rpm yielding film thickness L of approximately 150 nm. Aluminum contacts 100 nm thick were subsequently evaporated onto the polymer layer at pressures below 5×10^{-6} mbar covering both the conducting and the etched part of the ITO electrode. Electrical contacts were made by attaching copper wires to the ITO anode and the region of the aluminum cathode cov-

^{a)}Electronic mail: idws@st-andrews.ac.uk

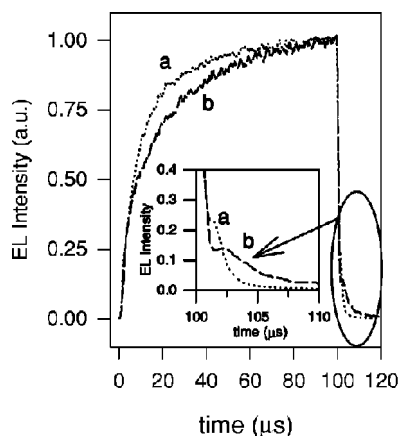


FIG. 1. EL transients of an ITO/MEH-PPV/Al device driven by 100 μ s pulses at (a) 295 K and 8 V, (b) 80 K and 9 V, normalized to the brightness at 100 μ s. Inset is the evolution of the EL after the driving bias has been switched off.

ering the etched ITO using silver paint. The LEDs had emissive areas of 7 mm². The samples were mounted in a liquid nitrogen cryostat under vacuum. The devices were driven electrically with a function generator with rise times <10 ns and the emission was detected by a photon counting setup with a multichannel analyzer. Typical RC times of the diode in the circuit were measured to be 600 ns, which is consistent with estimates based on the device geometry.

III. RESULTS

The EL response of the diodes to pulsed electrical excitation was recorded for different biases, pulse lengths, and temperatures. Figure 1 shows typical EL transients for a 100 μ s pulse at 295 and 80 K which are normalized to the maximum emission. At room temperature the pulse height V was 8 V, which was just enough to give an acceptable signal to noise ratio. As the device is cooled down, the turn-on field for light emission increases but so does the quantum efficiency, so at 80 K a bias of 9 V was chosen to give a comparable brightness. Figure 1 shows that the EL rise time increases as the temperature is lowered. This can be understood to arise from the slowing of minority carriers on the transition to dispersive transport observed at low temperatures.⁹ A remarkable feature is observed after switching off the voltage pulse as seen in the inset in Fig. 1. Initially, the EL decays rapidly corresponding to the discharging of the parallel plate capacitor the device represents. However, after a delay of 1–2 μ s, the EL is found to rise again and then decay slowly without the application of an external field. It can be seen that the total area of this overshoot and the position of the peak depend strongly on temperature.

We find that the overshoot also depends on pulse duration. A typical overshoot is shown in Fig. 2 for a 500 μ s pulse at 295 and 80 K. The EL initially decays rapidly and then rises again to a peak after 1.8 μ s at 295 K and 2.6 μ s at 80 K. We find that the overshoot is more pronounced for longer pulses. This can be seen by comparing Figs. 1 and 2. The lower panel of Fig. 2 shows the decay of the overshoot

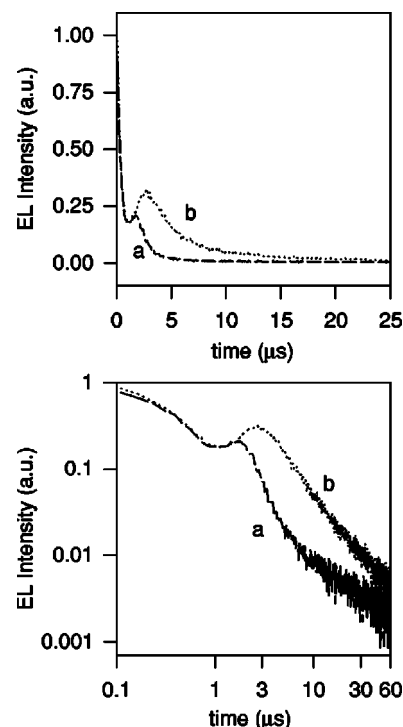


FIG. 2. Decay of EL after switching off the driving bias, normalized to the emission intensity at the point of turnoff (defined as time 0 μ s) for a 500 μ s pulse at (a) 295 K and 11 V and (b) 80 K and 12 V (upper panel). The lower panel shows the decay on a double logarithmic scale.

on a double logarithmic scale. The low temperature curve clearly decays according to a power law after the protrusion. The room temperature peak decays over the same time scale. However, it initially exhibits a more rapid decay than the low temperature measurement and then appears to slow down after approximately 10 μ s. The bias dependence of the overshoot is explored in Fig. 3 where EL traces of the device at 80 K are shown on a logarithmic scale at three different voltages. The intensity of the trace and the overshoot increase with applied bias. However, when normalized to the brightness at 100 μ s the peak of the overshoot and the decay times are unchanged, indicating that the applied bias has no

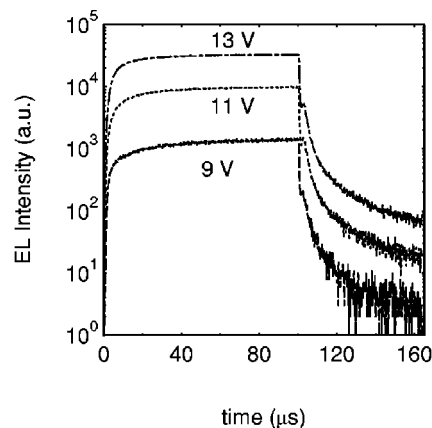


FIG. 3. Bias dependence of the transient EL features on a logarithmic scale at 80 K.

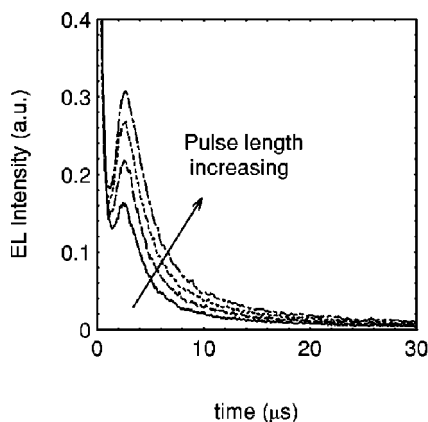


FIG. 4. Dependence of the delayed EL feature on pulse length at 12 V and 80 K (pulse lengths of 100, 200, 500, and 1000 μs).

effect on the physical dynamics of the overshoot other than to increase the number of charge carriers involved.

In contrast, there is a marked dependence of the area of the delayed recombination on pulse length, as shown in Fig. 4 for a device at 80 K driven with pulse lengths of 100, 200, 500, and 1000 μs with identical duty cycles of 10%. At room temperature, the peak area is smaller by a factor of 3.5, but the functional dependence is the same. The dependence of the integrated overshoot as a function of pulse length is shown in Fig. 5 in double logarithmic representation. The peak was integrated from the local minimum position at ~ 1 μs after turnoff. There is a small contribution from the normal decay of the EL, which is, however, orders of magnitude smaller than the overshoot at short times. It appears that the peak area increases with pulse length following a temperature independent power law with an exponent of ~ 0.3 . An increase in duty cycle was found to lead to a small increase in the peak area. Little dependence on duty cycle was observed below the 10% value used here, suggesting that this was sufficient to extract all of the trapped charge from the device prior to application of a new pulse.

Bilayer devices with polypyridine used as an electron transporting layer¹⁰ were also studied, but no overshoot was observed, indicating that the MEH-PPV—aluminum interface may be the origin of this effect. The delayed EL could be quenched completely by prebiasing the device with a con-

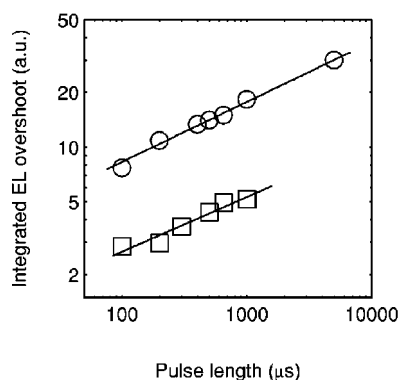


FIG. 5. Power-law scaling of integrated delayed EL feature with pulse length on a double logarithmic plot at 80 K (○) and 295 K (□).

stant 2 V dc offset. The overshoot peak was also found to disappear when the device was operated in air, which suggests that the trapping of charges is not due to atmospheric impurities introduced into the polymer during processing.

IV. DISCUSSION

A. Qualitative interpretation

Overshoot effects have previously been discussed in both single^{2,6} and bilayer devices.⁵ In many cases, overshoots are associated with large currents or even sparking⁶ and occur directly after switching off the bias. A similar effect to the one observed here has been noted by Pinner *et al.*,^{2,11} although the EL hump observed occurs with a delay on time scales in the order of milliseconds² or 10 μs .¹¹ A preliminary qualitative discussion² and quantitative analysis¹¹ linked the phenomenon to interfacial effects and strong local electric field gradients under the space charge limited conditions of carrier flow. In contrast, in our ITO/MEH-PPV/Al structure, both electron and hole currents are injection limited. The overshoot effect in bilayer LEDs has been discussed and modeled in detail by Nikitenko *et al.*⁵ Qualitatively, we find that our results for single layers are similar to those reported previously, although the brightness of the anomaly reported here does not exceed the brightness prior to switching off the bias. However, the fact that the effect reported here is observed in a single layer device with non-ohmic contacts suggests that the origin is due not to high spatial gradients of electric field or charge accumulation at a polymer/polymer interface, but to charge trapping at the polymer/metal interface. We propose, as an extension of the scenario previously described in Ref. 2, a superposition of detrapping of charge carriers and quenching of singlet excitons at the metal cathode to explain the shape of the protrusion and its distinct separation from the switchoff region of the EL trace.

The polymer/aluminum interface plays a crucial role in device operation. First, a thin insulating aluminum oxide layer between the polymer and the metal would lead to significant buildup of positive space charge at the cathode. Second, majority charge carriers may be trapped at the *n*-doped polymer/aluminum interface^{12–14} during device operation due to the presence of metallic atoms. The influence of positive space charge on the injection of minority carriers is important, as the barrier to injection from aluminum into MEH-PPV is very high. It appears that the trapping process depends on the length of the current pulse rather than the magnitude, as is seen in the comparison of Figs. 3 and 5. A schematic representation of the processes giving rise to the overshoot is shown in Fig. 6. When the bias is turned off, the holes are sucked back into the anode as the parallel plate capacitor discharges with the characteristic RC time constant. Some majority carriers, however, remain trapped at the metal/polymer interface, whereas some minority carriers are still trapped in the bulk^{15–17} of the device after turnoff ($t = 0$). The field inside the LED then approaches zero (at $t \geq 1$ μs), and holes migrate back to the anode and recombine with electrons they meet on the way. As luminescence is effectively quenched within 10 nm of the metal,¹⁸ the de-

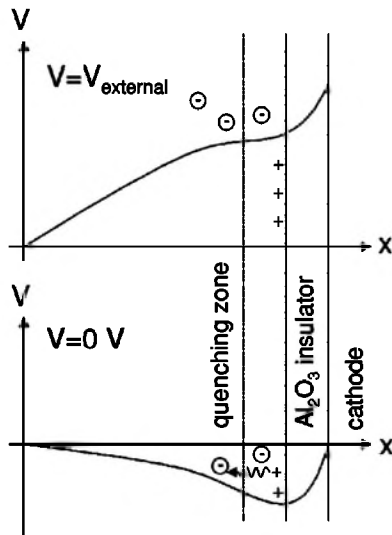


FIG. 6. Schematics of the processes giving rise to the overshoot. Under application of an external bias holes are accumulated at a thin insulating layer between the cathode and the polymer. Upon switching off the bias, the internal field is reversed and holes migrate back to the anode and meet up with electrons in the bulk of the material. The luminescence is quenched within a characteristic quenching zone in the region of the cathode.

trapped charge carriers have to migrate a certain distance before radiative recombination can occur. This, in qualitative terms, is the origin of the delayed luminescence peak. Since the delay itself is governed by the diffusion of holes, the temporal position of the delayed luminescence peak does not depend on pulse length or bias at $t < 0$. The absence of a bias dependence suggests that injection effects are not relevant to the overshoot process. Application of a 2 V dc bias offset quenches the delayed luminescence because in this case the internal field cannot reverse, and holes hence cannot be released from the cathodic trapping surface.

B. Charge carrier diffusion

Since the energy barriers for hole and electron injection are ~ 0.5 and ~ 1 eV,^{19,20} respectively, the transport is, in general, injection limited. Consequently, the electric field and the spatial density of holes are uniform, $F_0 = V/L$ and $p(x, t) \approx p_0$. The uniformity also results from the predominance of holes inside the LED, while the density of electrons decreases sharply with the distance from the cathode, x , due to recombination on a scale of the order of a few nanometers.²⁰ Accounting for the suppression of radiative recombination at $x < a_0$ due to singlet exciton quenching, a_0 being the effective quenching distance from the cathode of the order of 10 nm, the quasistationary (st) EL current at $t = 0$ can be expressed as follows:

$$J_{\text{EL}}^{\text{st}} = \varphi_0 R_L p_0 \Sigma_e, \quad (1)$$

where φ_0 is the average efficiency of radiative recombination at $x > a_0$, Σ_e is the area density of electrons in the region of most effective EL (at $x \geq a_0$), and the Langevin recombination constant $R_L = e\mu_h/\varepsilon\varepsilon_0$ which is governed by the field-dependent mobility of holes $\mu_h(F_0)$ (e is the elementary charge, ε_0 is the permittivity of free space, and ε is the

dielectric constant of the polymer, which is taken to be 3). We assume that the hole mobility considerably exceeds the electron mobility in the field ranges under consideration.

The existence of a blocking layer on the cathode leads to the formation of a surface density of holes $\Sigma \approx J_h/\omega$, ω being the hole tunneling frequency and $J_h = \mu_h F_0 p_0$ the hole current. It should be noted that for the case of zero bias, the potential drop between the anode and the position of interfacial holes is less than 0.5 V, even if the hole area charge density $e\Sigma$ is comparable to capacitor area charge density $\varepsilon\varepsilon_0 F_0$. This is a consequence of the proximity of interfacial holes to the anode. The time period $t \approx 1 \mu\text{s} \gg RC$ is sufficient for the majority of holes in the bulk to saturate the interfacial layer or escape from the LED. Thus, the diffusion rather than drift of “cathodic” holes, i.e., holes accumulated at the cathode, in their own electric field towards the anode is responsible for the spike. The holes located at the interface can be divided quantitatively into “hot” (mobile) holes with mobilities approaching μ_h , and “cold” holes, localized on deeper interfacial states, with much smaller mobilities. The “hot” holes are found to be responsible for the EL spike itself and for the initial decay of EL after the spike. Indeed, even if the diffusion coefficient of “hot” holes corresponds to a value of mobility as high as $\mu_{h0} \approx 10^{-5} \text{ cm}^2/\text{Vs}$, the carriers diffuse a distance 5–10 nm, comparable to the quenching distance a_0 , within 1–2 μs after the moment of the EL minimum at $t \approx 1 \mu\text{s}$. Similar time scales are observed experimentally.

The analyses of the overshoot kinetics requires, however, more detailed consideration. The time required by the electrons to spread to their quasistationary spatial distribution (i.e., the recombination lifetime) can be estimated from the saturation time of EL (see Fig. 1). It is not shorter than 20 μs at $T = 295 \text{ K}$ and larger at $T = 80 \text{ K}$. The electron density on a time scale $t \leq 20 \mu\text{s}$ after switching off the bias is, consequently, the same as prior to the end of the bias pulse. Since the EL spike is substantially less bright than the EL at $t \leq 0$, the recombination time of electrons at $t > 0$ exceeds 20 μs considerably. Thus, the majority of electrons survive on the time scales considered here. Hence the kinetics of the EL decay are completely determined by the hole diffusion, and since in the limit of diffusion controlled decay $J_{\text{EL}} \sim t^{-0.5}$, the decay is asymptotic. Experimentally, however, a power-law decay with the average temperature-independent exponent -1.65 is observed, as seen in Fig. 6.

C. Geminate recombination of correlated electron-hole pairs

The observed kinetics of the EL decay can be rationalized in terms of geminate recombination (GR) of electron-hole pairs²¹ near the cathode. After turnoff of the voltage pulse, the injected charge carriers are removed from the device, leaving the Coulombically bound geminate pairs. The process of geminate recombination is also controlled by diffusion of the fastest carrier in a pair, but it is accelerated by the mutual Coulomb field. It is well known²² that the GR-controlled recombination rate ($-dW/dt$) at a time t after a spike decreases according to a temperature-independent power-law $t^{-2 \dots -1.5}$ with the exponent gradually changing

from approximately -2 to -1.5 , where $W(t)$ is the survival probability of the geminate pair generated at $t=0$. The GR-controlled reaction rate is strongly affected by the initial separation of the pair $r_0 < r_c$, where $r_c = e^2/4\pi\epsilon\epsilon_0 kT$ is the Onsager (Coulomb) radius, $r_c(T=295\text{ K}) \approx 17\text{ nm}$ and $r_c(T=80\text{ K}) \approx 63\text{ nm}$. This radius considerably exceeds the distance between some of the interfacial holes and the majority of “radiative” electrons, which can recombine radiatively. However, GR is meaningful as a specific way of recombination only if the majority of recombining pairs have spatial separations less than r_c , i.e., if pairs are spatially correlated. Otherwise, an equation of the type (1) invoking the Langevin constant is the adequate way of describing the carrier recombination. “Hot” holes in the proximity of the interface are located preferentially inside the Coulomb sphere of an electron. This results from the perturbing influence of the electric field lines around the electron on the hole as well as the influence of the blocking layer, which acts as a reflecting boundary for holes. The probability of hole capture inside a planar potential well of radius $\sqrt{r_c^2 - x^2}$ ($x < r_c$ being the distance of an electron from the blocking layer) during the time period smaller or comparable to the recombination lifetime of electrons is close to unity. This means that the average number of correlated “hot” holes per “radiative” electrons is governed by the ballistic Coulomb capture cross section $e/\epsilon\epsilon_0 F_0$ rather than r_c^2 . The probability of holes appearing on the interface at a distance smaller than r_c from “radiative” electrons during the time period smaller or comparable to the recombination lifetime of electrons (at $t < 0$) is of the same order as the probability of recombination, i.e., close to unity. The potential well, formed on the cathode surface by the Coulomb field of localized carriers, reduces the probability of hole capture on a deep interfacial state, provided there is no such state inside the well, and increases the probability for the hole to remain “hot” until the bias is switched off. Otherwise, if the captured hole became trapped and hence “cold,” its Coulomb repulsion would suppress recombination of an electron with other noncorrelated “hot” holes on an initial time scale at $t > 0$.

Using Eq. (1), one obtains for the normalized GR-controlled EL current at $t > 0$

$$\frac{J_{\text{EL}}(t)}{J_{\text{EL}}^{\text{st}}} = \frac{N(r_0, r_c) \epsilon \epsilon_0 F_0}{e J_h(F_0)} \left(-\frac{\partial W(r_0, t)}{\partial t} \right), \quad (2)$$

where $N \ll 1$ is the average number of correlated “hot” holes per “radiative” electron, which quantifies the trapping process. Due to the lack of experimental information on the spatial and energetic distribution of the traps, this correlation parameter N is chosen as the free parameter in the model. The lower limit for r_0 in Eq. (2) is the distance of total EL quenching $a_0 \leq 10\text{ nm}$. The rigorous solution for the GR-controlled recombination rate at $t > 0$ is complicated by the following circumstances: (1) The initial distribution of holes relative to electrons is not spherically symmetric; (2) the oxide blocking layer acts as a weakly absorbing surface for the holes; (3) the initial separation of different pairs is not constant; (4) even for the simplest case of an initial distribution of holes on a sphere of radius r_0 centered around an electron the exact mathematical solution is very complicated.²³ How-

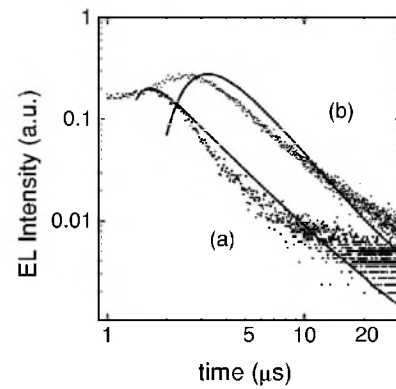


FIG. 7. EL overshoot kinetics after a 500 μs pulse at (a) 295 K and (b) 80 K. The points are experimental data and the solid lines are calculated from Eq. (2). The parameters used are $\mu_{h0} = 8 \times 10^{-6}\text{ cm}^2/\text{V s}$, $\epsilon = 3$, (a) $J_h = 5\text{ mA}/\text{cm}^2$, $N = 0.020$, $V = 11\text{ V}$; (b) $J_h = 1\text{ mA}/\text{cm}^2$, $N = 0.026$, $V = 12\text{ V}$.

ever, for the qualitative description of the GR rate, the simple “prescribed diffusion approximation”²² is applicable. The result for the spherically symmetric initial distribution is $W(r_0, t) = \exp(-(r_c/r_0)\{1 - \text{erf}(r_0/\sqrt{4\pi Dt})\})$ where D is the diffusion coefficient and erf is the error function.

Figure 7 shows that the results of calculations from Eq. (2) and experimental data at $T=295\text{ K}$ and $T=80\text{ K}$ are in qualitative agreement. The average calculated exponent of the EL decay at $T=80\text{ K}$ is -2 , and the time at which the spike occurs is somewhat overestimated by the model. This overestimate is due to the prescribed diffusion approximation used above and is more significant at low temperature.²³ The broadening of the experimental maximum at short times can be associated with the recombination of the pairs with shorter initial separations. Detrapping of “cold” holes or recombination of noncorrelated pairs can be responsible for the long-lived EL tail for $t \geq 20\text{ }\mu\text{s}$, especially at high temperature. The values of the average initial separations r_0 (10 nm at 295 K and 11.5 nm at 80 K) are close to the distance of effective quenching of radiative recombination by the metal electrode. The number of “hot” correlated holes per electron N (0.026 at 295 K and 0.020 at 80 K) is much less than unity. Thus, the majority of electrons survive initially, as was mentioned above.

A relatively weak temperature dependence of the magnitudes and times of the spike are a striking feature of the experimental results. It should be noted that the increase of the Coulomb acceleration of GR, which is reflected in the increase of r_c/r_0 with decreasing temperature, partially compensates for the decrease of the diffusion coefficient. The latter is related to the mobility of “hot” holes μ_{h0} through the Einstein relation $D = \mu_{h0} kT/e$. The weak temperature dependence and high value of this mobility (it is assumed to be $8 \times 10^{-6}\text{ cm}^2/\text{V s}$ at both temperatures) can be rationalized by realizing that this quantity is actually effectively increased by the Coulomb field and is hence not the real temperature-dependent zero-field mobility.

As commented on above, the application of an external dc bias of 2 V quenches the delayed luminescence. The built-in potential is estimated as being the difference in the electrode work functions and is of the order of 0.5 V. With a

sample thickness of $L = 150$ nm, one hence obtains a field of $F_0 = 10^5$ V/cm. Assuming an initial separation of geminate pairs of $r_0 = 10$ nm, one finds that eF_0r_0/kT is close to 4, which is considerably greater than unity. GR is hence suppressed.²³ In comparison, the contribution of the built-in field to GR is relatively small and acts as an accelerator to diffusion.

D. Area of the delayed luminescence peak

The area of the delayed luminescence peak can be derived from Eq. (2). Integrating with respect to time yields

$$Q = \frac{N(r_0, r_c) \epsilon \epsilon_0 F_0}{e J_h(F_0)} [1 - W_\infty(r_0)], \quad (3)$$

where $W_\infty(r_0) = \exp(-r_c/r_0) \ll 1$ is the escape probability from GR. Since $N \sim \Sigma \sim J_h(F_0)$, and N is correlated with the Coulomb capture cross section $e/\epsilon \epsilon_0 F_0$, the integral of the relative EL spike Q defined by Eq. (3) appears to be field independent. This is consistent with the experimental observations in Fig. 3. This field independence of the EL kinetics is also apparent from Eq. (2), as $W(r_0, t)$ is not field dependent.

The interesting and striking feature of the dependence of Q on the pulse length is its invariance with temperature. A similar effect has been observed and investigated in double-layer structures.⁵ It was attributed to the progressive accumulation of minority carriers (electrons) at the internal polymer–polymer interface.⁵ The difference to the present case is, however, that there is no significant electric field inside the LED after switching off the external bias. Also, electrons are immobile on the time scale under consideration and the majority of electrons are conserved after the spike (recall that the overshoot effect is much smaller than in the case of the previous work⁵). Progressive accumulation of electrons near the cathode was also shown to influence the experimental results in Ref. 5, resulting in the gradual increase of EL at long times under application of a bias, as is seen in Fig. 1. However, in the present investigation the increase of Q with pulse length is much stronger than in Ref. 5. On the other hand, from the results in Fig. 5 the progressive increase of the total area density of interfacial holes requires a lifetime of carriers inside the LED of more than $10^4 \mu\text{s}$, which is hardly compatible with the model described above or the relatively small value of Q . However, the total density of interfacial holes significantly exceeds that of “hot” holes, and the increase of the overshoot effect with pulse length may be rationalized qualitatively as the increase of the fraction of the “hot” holes with time (at $t < 0$). A similar phenomenon (i.e., the increase of the fraction of mobile carriers under continuous generation) is well known in the situation of nonequilibrium carrier kinetics resulting in dispersive transport (see, for example, Refs. 16 and 24). The latter process results from thermalization within a broad energy distribution of localized states and is, in contrast, strongly dependent on temperature.

The increase of the fraction of mobile carriers with time under continuous generation, resulting from the thermalization within a broad energy distribution of localized states is,

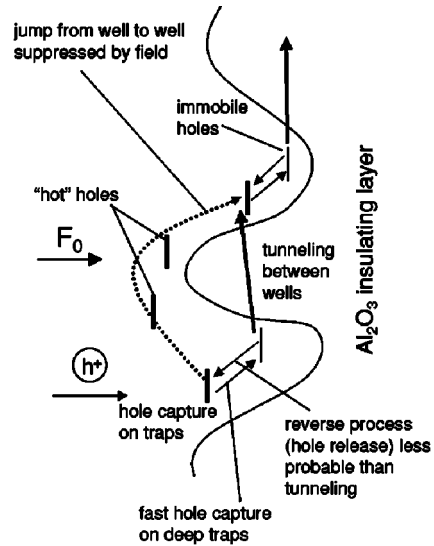


FIG. 8. Schematics of hole trapping and release at the cathode. Due to the surface roughness of the insulating aluminum oxide layer between the polymer and the cathode, potential wells are formed which act as hole traps. Holes are either mobile (“hot,” marked by bold lines) or are trapped in the surface wells and are immobile (thin lines). Thermally activated jumps between wells are suppressed by the external field. Carriers are hence rapidly captured on traps. As the reverse release processes are thought to be less probable, tunneling transitions between wells form the rate limiting steps.

in contrast, strongly affected by the temperature. The weak temperature dependence of the EL overshoot kinetics observed in Ref. 5 was previously explained by attributing the origin of the overshoot process to positional rather than energetic disorder of the rate-limiting states. This interpretation also applies to our current investigation. It should be noted that the thermalization kinetics of interfacial holes are strongly affected not only by the energy distribution of interfacial traps, but also by spatial features of the surface of the blocking layer and possible unevenness. The effect of surface roughness on carrier localization is described schematically in Fig. 8. Particularly in the case of a strong electric field of $F_0 \approx 10^6$ V/cm, such a roughness could lead to the suppression of diffusion in the direction opposite to that of the field. Clusters of several neighboring surface traps, which we describe in terms of surface wells, would hence be relatively isolated from other clusters by barriers of insulating Al_2O_3 and give rise to features which result in “dispersive” kinetics of localized carriers. These features are first that the release from a cluster is much more difficult for a carrier than the capture of a carrier on a trapping state in a cluster, and second, that the release times are broadly distributed. A temperature independence of the relaxation of “hot” carriers is hence a signature that tunneling between different clusters in the plane of the surface, i.e., orthogonal to the field direction, is the rate limiting step, rather than thermalization within a cluster. In the case of a sharp decrease in the distribution of interfacial traps with energy, one concludes that the majority of interfacial holes generated are initially in a “hot” state.

If the release time t_r is controlled by the energy of a trapping state E , giving $t_r \sim \exp(E/kT)$, and the energies are distributed exponentially according to $g(E) \sim \exp(-E/E_0)$, it

is known that the fraction of mobile (“hot”) carriers decreases with time as $(t-t')^{\alpha-1}$, where $\alpha=kT/E_0$ is the dispersion parameter and t' is the time of generation.^{24,25} In the present case the release time is controlled by the tunneling length r , so $t_r \sim \exp(2r/a_s)$, a_s being the localization length of the carriers in the direction along the surface of the blocking layer. The distribution of tunneling lengths in the direction of nearest proximity of neighboring surface wells is adequately described by the one-dimensional Poisson equation $\Phi(r) \sim \exp(-r/d)$, using the characteristic length d . The similarity between the functional forms of these two equations leads to the conclusion that this distribution of tunneling lengths provides the same energetic relaxation kinetics of “hot” holes which would result from thermalization of carriers in an exponential energy distribution of traps.¹⁶ By means of this analogy, and assuming that t is equal to the pulse length P , integration of the fraction of mobile (“hot”) carriers over t' from 0 to P yields the power-law observed in Fig. 5:

$$Q \sim N \sim P^\alpha, \quad \alpha = a_s/2d. \quad (4)$$

The straight lines in Fig. 5 show the excellent fit of the functional form in Eq. (4) to the experimental data at $T = 295$ K and $T = 80$ K with $\alpha \approx 0.3$. It should be noted that the localization length of a carrier a_s is much larger in a strongly bonded inorganic solid such as Al_2O_3 than in a van der Waals bonded organic.²⁶ Assuming $a_s \approx 1$ nm, one obtains $\alpha = 0.3$ at the reasonably large value of $d \approx 1.5$ nm. Using the same parameters as for the fit in Fig. 7, the ratio of the absolute values of Q for the two temperatures, as calculated from Eq. (3), is found to be 5. Considering the qualitative character of the model, this value is remarkably close to the experimental value of 3.5 seen in Fig. 5.

V. CONCLUSIONS

We have reported the appearance of a time delayed overshoot in single layer MEH-PPV LEDs. The phenomenon can be explained by considering the effect of a thin insulating barrier layer between the cathode and the polymer and taking into account the effect of spatial correlations of electrons and holes on the diffusion of charge carriers. The fact that the decay of the luminescence is offset somewhat from the time of current turnoff is a signature of the electrode quenching of excitations formed in the vicinity of the cathode. We attribute the creation of trapping sites to a modification of the polymer at the metal/polymer interface and not to the bulk of the sample, as the observed protrusion disappears after oxidation of the polymer and is not observed in bilayer devices. Clearly, an accumulation of charge as observed here will lead to a modification of the device capacitance and could well contribute to transient measurements of capacitance and conductance.^{16,17} Our measurements hence provide a possible explanation of previous transient measurements,¹⁶ which appear to be in conflict with the observation that most device properties such as current-voltage characteristics and efficiency may be explained without the need to include trapping effects.^{9,19,27,28} We have shown that transient EL provides an extremely useful tool to probe the device properties

and can be used to gain microscopic insight into carrier kinetics using appropriate models. Finally, the observation of relatively long decay transients in these devices and the occurrence of delayed luminescence are of considerable importance for display applications. In passively addressed displays, the luminescence lifetime is clearly of importance and any increase in lifetime will lead to a reduction in apparent flicker. The controlled introduction of trapping and charge accumulation sites may hence increase the performance of passive matrix displays and should be explored further.

ACKNOWLEDGMENTS

The authors thank EPSRC and Raychem Ltd. for financial assistance as well as Covion GmbH for the supply of MEH-PPV. I.D.W.S. is a Royal Society University Research Fellow. J.M.L. thanks the German Academic Exchange Service for funding a trip to Marburg and K. Book for helpful discussions. V.R.N. thanks the Deutsche Forschungsgemeinschaft (Project Nos. 436 RUS 113/9314 and BA 411/33-3).

- ¹R. H. Friend, R. W. Gymer, A. B. Holmes, J. H. Burroughes, R. N. Marks, C. Taliani, D. D. C. Bradley, D. A. DosSantos, J. L. Brédas, M. Logdlund, and W. R. Salaneck, *Nature (London)* **397**, 121 (1999).
- ²D. J. Pinner, R. H. Friend, and N. Tessler, *J. Appl. Phys.* **86**, 5116 (1999).
- ³J. Pommerehne, H. Vestweber, Y. H. Tak, and H. Bässler, *Synth. Met.* **76**, 67 (1996).
- ⁴D. Braun, D. Moses, C. Zhang, and A. J. Heeger, *Synth. Met.* **55–57**, 4145 (1993).
- ⁵V. R. Nikitenko, V. I. Arkhipov, Y. H. Tak, J. Pommerehne, H. Bässler, and H. H. Horhold, *J. Appl. Phys.* **81**, 7514 (1997).
- ⁶V. Savvateev, A. Yakimov, and D. Davidov, *Adv. Mater.* **11**, 319 (1999).
- ⁷N. Tessler, N. T. Harrison, and R. H. Friend, *Adv. Mater.* **10**, 64 (1998).
- ⁸P. W. M. Blom and M. Vissenberg, *Phys. Rev. Lett.* **80**, 3819 (1998).
- ⁹I. H. Campbell, D. L. Smith, C. J. Neef, and J. P. Ferraris, *Appl. Phys. Lett.* **74**, 2809 (1999).
- ¹⁰S. Dailey, M. Halim, E. Rebourt, L. E. Horsburgh, I. D. W. Samuel, and A. P. Monkman, *J. Phys. CM* **10**, 5171 (1998).
- ¹¹D. J. Pinner, R. H. Friend, and N. Tessler, *Appl. Phys. Lett.* **76**, 1137 (2000).
- ¹²J. M. Bharathan and Y. Yang, *J. Appl. Phys.* **84**, 3207 (1998).
- ¹³W. R. Salaneck, *Philos. Trans. R. Soc. London, Ser. A* **355**, 789 (1997).
- ¹⁴P. Dannetun, M. Logdlund, M. Fahlman, M. Boman, S. Stafstrom, W. R. Salaneck, R. Lazzaroni, C. Fredriksson, J. L. Brédas, S. Graham, R. H. Friend, A. B. Holmes, R. Zamboni, and C. Taliani, *Synth. Met.* **55**, 212 (1993).
- ¹⁵P. W. M. Blom, M. J. M. Dejong, and J. J. M. Vleggaar, *Appl. Phys. Lett.* **68**, 3308 (1996).
- ¹⁶A. J. Campbell, D. D. C. Bradley, and D. G. Lidzey, *J. Appl. Phys.* **82**, 6326 (1997).
- ¹⁷J. Scherbel, P. H. Nguyen, G. Paasch, W. Brutting, and M. Schwoerer, *J. Appl. Phys.* **83**, 5045 (1998).
- ¹⁸H. Becker, S. E. Burns, and R. H. Friend, *Phys. Rev. B* **56**, 1893 (1997).
- ¹⁹J. M. Lupton and I. D. W. Samuel, *J. Phys. D* **32**, 2973 (1999).
- ²⁰B. K. Crone, I. H. Campbell, P. S. Davids, D. L. Smith, C. J. Neef, and J. P. Ferraris, *J. Appl. Phys.* **86**, 5767 (1999).
- ²¹D. M. Pai, in *Physics of Disordered Materials*, edited by D. Adler (Plenum, New York, 1985).
- ²²A. Mozumder, *J. Chem. Phys.* **48**, 1659 (1968).
- ²³K. M. Hong and J. Noolandi, *J. Chem. Phys.* **68**, 5163 (1978).
- ²⁴V. I. Arkhipov and H. Bässler, *Philos. Mag. B* **68**, 425 (1993).
- ²⁵V. I. Arkhipov and A. I. Rudenko, *Philos. Mag. B* **45**, 189 (1982).
- ²⁶U. Wolf and H. Bässler, *Appl. Phys. Lett.* **74**, 3848 (1999).
- ²⁷L. Bozano, S. A. Carter, J. C. Scott, G. G. Malliaras, and P. J. Brock, *Appl. Phys. Lett.* **74**, 1132 (1999).
- ²⁸A. Ioannidis, E. Forsythe, Y. L. Gao, M. W. Wu, and E. M. Conwell, *Appl. Phys. Lett.* **72**, 3038 (1998).